Comparative evaluation of the performance of a capacitive and a non-capacitive microbial fuel cell

[1,3] Imologie Meshack Simeon
[1]Department of Agricultural and Bioresources, Federal University of Technology, Minna, Nigeria
ORCID: 0000-0003-1412-3215
s.imologie@futminna.edu.ng

Agbotiname Lucky Imoize
[2]Institute of Digital Communication, Department of Electrical Engineering and Information Technology, Ruhr University, Bochum 44801, Germany.
aimoize@unilag.edu.ng

Ruth Freitag
[3]Chair of process Biotechnology, Faculty of Engineering science, University of Bayreuth, Germany;
bioprozesstechnik@uni-bayreuth.de

Abstract— **Electrode materials play a critical role in the performance of microbial fuel cells. This study investigates the contribution of capacitive bio-electrodes to sustainable power production in a single-chamber microbial fuel cell (MFC). The capacitive electrodes consisted of a stainless-steel wire mesh with an activated carbon layer, while the non-capacitive control electrodes were made of graphite felt with a wound current collector. The MFCs were constructed using a glass vessel with the anode completely buried in biologically active soil and the cathode placed above the soil to form a single chamber configuration. The performance of the MFCs was investigated using linear sweep voltammetry (LSV) and electrochemical impedance spectroscopy (EIS). The results showed that the performance of the capacitive MFC was three times better than that of the non-capacitive MFC. While there was no significant difference in the Ohmic resistances of the MFCs, there was a significant difference in charge transfer resistance and capacitance of the MFCs. The capacitive MFC had a double layer capacitance of 8.282 µF in addition to the diffuse layer capacitance at the layer/metal interface of 2.012 F, while the non-capacitive MFC had a double layer capacitance of 5.034 µF with no diffuse layer capacitance. The results show that the capacitive characteristics of both cathode and anode improve the performance of a single-chamber MFC.**

Keywords—capacitive MFC, electrodes, power, resistance, microbial fuel cell.

I. Introduction

Microbial fuel cell (MFC) technology uses the natural metabolism of electroactive microbes to generate electricity. This technology represents one of the fastest-growing renewable energy technologies in the last decade owing to the fascinating possibilities of MFCs to treat wastes while generating bioelectricity through bacterial metabolism [1] Apart from being environmentally friendly, MFC technology enables the direct conversion of substrate energy into electricity, thus ensuring the conversion of waste into energy [2–4]. Therefore, the efficiency of MFCs is considered relatively high compared to other bio-electrochemical technologies because no input energy is required. However, their low power density and fluctuations due to the natural activities of the Electroactive bacteria (EAB) still pose limitations for their real-world applications [5]. Therefore, improved performance of MFCs requires, among other things, optimization of the architectural aspect.

The fundamental components of interest in the design and construction of MFCs are electrodes (cathode and anode), wiring, cell vessel(s), and exchange Membrane. MFCs are built from a variety of materials and in an ever-increasing variety of configurations. Since the redox reaction in MFCs occurs at the electrodes, special consideration of electrode materials is required in the design of MFCs. A good electrode material must be bio-compatible, conductive, non-corrosive, non-fouling, porous, inexpensive, easy to manufacture, applicable to larger systems, and have a large surface area [6] to improve the metabolism of the associated EAB. Carbon-based electrodes are most commonly used in MFC research because they meet much of the criteria for good electrode materials [6]. Carbon electrodes are available as compact graphite sheets, rods, or granules, as fibrous materials (felt, cloth, paper, fibres, foam), and as glassy carbon [6,7]. The most common materials for the anode

are graphite sheets or rods because they are relatively cheap, easy to handle, and have a well-defined surface [8–10]. Conductivity is one of the most important attributes of these materials because electrons must flow through the material from the point of transfer by the microorganism to the collection point. While many metals fit this important characteristic, they fall short in applicability due to their corrosive nature and lack of a suitable surface for bacteria attachment [11]. Non-corrosive stainless steel mesh is common as a metal-based composite electrode in MFCs, but copper is barely used due to its antibacterial properties in aqueous environments [12,13]

The application of electrodes made of metals and metal-based materials to improve MFC performance has been extensively researched. Among other metals, stainless steel (SS) has emerged as an excellent alternative electrode material to pure carbon-based electrodes due to the excellent mechanical properties, electrical conductivity and corrosion resistance of high quality SS materials; coupled with its unique easy scalability and stability for long-term operation of MFCs [8,14]. However, although SS is an efficient electrode capable of producing stable current densities, it is not often used in its pure form because it does not have sufficient surface area for robust biofilm development. Therefore, improvement in the performance of the SS electrode is achieved by surface modification [15]. The most common surface modification of SS electrodes is coating with carbon-based nanomaterials. [16,17]. These materials have excellent properties, such as increasing the number of active reaction sites for bacteria, greater opportunities for bacterial attachment, increased bacterial biocatalytic activities with a consequent increase in power densities [18]. Besides, the surface coating of SS electrodes has been reported to improve their capacitive properties, thereby increasing the overall performance of MFCs [19].

The use of external capacitors is known to be effective in slightly increasing the output power of MFCs to drive devices that require higher power than the MFCs can normally produce [20,21]. This is possible by connecting the MFCs to charge capacitors to provide short power spikes that are slowly recharged by the MFCs [22]. Thus, charges can be stored by the capacitors and intermittently delivered at a higher level than the power output of the MFC. In addition to external capacitors, recent studies have shown that the use of electrode materials with electrochemical capacitive properties can improve MFC current generation [15,23]. This is due to their high specific surface area [24] , which enables charge storage with the formation of an electrical double layer (EDL). Thus, a capacitive electrode improves the internal capacitance of an MFC leading to increased power quality [25]. Capacitive electrode materials with a high specific surface area are advantageous in MFCs due to their particular ability to reduce the overpotentials of MFCs and thus increase the overall power density [26–29].

Currently, there is a rise in the number of studies that utilize capacitive materials as electrodes in MFCs. However, most of the studies only consider one electrode at a time. Since the anode is considered the hub of bacterial activities leading to the transfer of electrons in MFCs, most studies are focused on the development of capacitive bio-anodes [2,19,30–32]. A few studies have also reported the importance of capacitive biocathode on the overall performance of MFCs [16,33]. Considering the anode and cathode of an MFC as two pseudo-capacitors in series, high cell capacitance could be achieved when both electrodes possess capacitive features [26].

This study evaluated the contributions of the combined capacitive properties of anode and cathode to the overall performance of a single-chamber microbial fuel cell catalysed by soil microbes. The performance of an MFC fabricated with both electrodes made of capacitive granular carbon material was compared to a control MFC with electrodes made of carbon fibres materials that lack capacitive properties.

II. Materials and Methods

A. Production of Capacitive Electrodes.

The Capacitive electrodes were developed by integrating a stainless-steel wire mesh, an activated carbon catalyst layer, and a binder into one unit. The adhesive paste was prepared from a 2-component epoxy adhesive (UHU plus Endfeet, Germany) by mixing the same amount (2.7 g) of binder and hardener. To improve the capacitive and the conductive properties of the paste, 0.25 g of carbon black (Vulcan XC-72) was added and thoroughly mixed. The mixture was then applied evenly and thinly to a clean stainless-steel mesh (type 1.4301, Germany) with a mesh size of 0.315 mm and a wire gauge of 0.2 mm. The electrodes were further coated with a layer of carbon black [34] (Fig. 2A) to increase the surface area and pressed overnight with screw clamps between two planes. The dry weight of the applied capacitive paste was 2.15 g, while the final weight of each electrode without the extended current collector for external circuit connection was 5.7

± 0.4 grams. The non-capacitive control electrodes (both anode and cathode) were made of carbon felt (AvCarb C100 Soft Carbon Battery Felt) (Fig. 2B). A titanium wire current collector with a diameter of 0.5 mm and a purity of 99.9% was inserted into the carbon felt and firmly fixed on both sides with the adhesive paste to ensure good electrical contact. All exposed current collectors were insulated with heat shrink tubing (0.32 - 0.16 cm)

B. MFC Construction and Operation

The MFCs were constructed around cylindrical glass vessels (Fig. 1) as previously described [35]. A mixture of garden compost and topsoil for agricultural cultivation, saturated with distilled water, was used as the source of the inoculum, ion exchange membrane, and nutrient-rich electrolyte [36] . Artificial wastewater, prepared according to [37], was used to occasionally enrich the medium with a substrate, for continuous bacterial metabolism. The MFCs were set-up in duplicates.
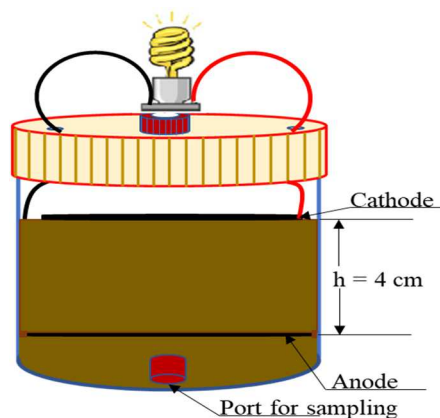

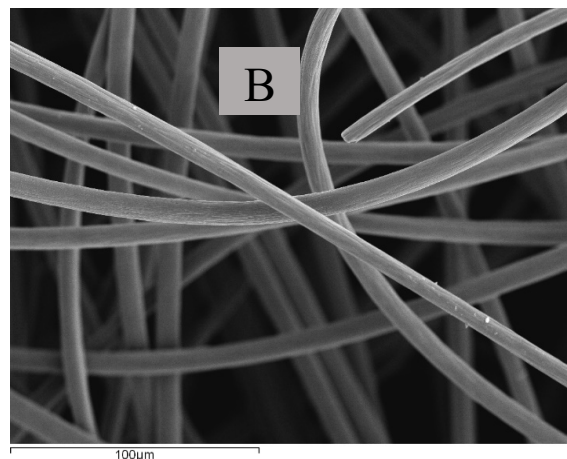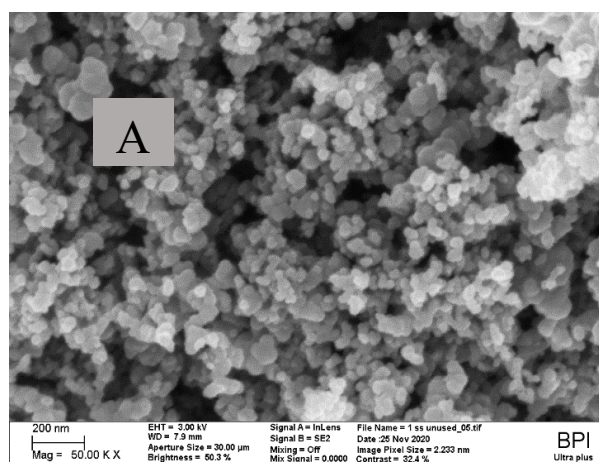Fig. 1. Schematic Set-up of the Single-Chamber MFC

Fig. 2. SEM images showing the structures of the Capacitive (A) and non-capacitive (B) electrodes before use.

C. Data collection and electrochemical characterization of the MFCs

The electrical outputs of the MFCs were recorded every 1 hour by a data logger (ADC-24, Pico Technology). Biofilm growth was monitored by open-circuit voltage (OCV). Electrochemical characterization of the cells was performed in a two-electrode system using a potentiostat (Biologic VMP3). Polarization curves were obtained by linear sweep voltammetry between open-circuit and zero potentials at a scan rate of 1 mV/s. Characterization of the capacitance and resistance of the MFCs was performed by electrochemical impedance spectroscopy (EIS). All EIS experiments were performed in a potentiostatic mode at an amplitude of 10 mV/s and a frequency range of 100 kHz to 10 mHz [38]. The values of the capacitance and the resistance were obtained from Nyquist plots by fitting the EIS to an equivalent electrical circuit [39] using EC-lab.

III. RESULTS AND DISCUSSIONS

Comparative evaluation of the capacitive (MFC_c) and non-capacitive (MFC_{nc}) MFCs was performed using various techniques. These include continuous open-circuit voltage measurement with a data logger (ADC-24), linear sweep voltammetry (LSV) to extract the maximum power point of the MFCs over time, and electrochemical impedance spectroscopy (EIS) to simulate the capacitive and resistive characteristics.

A. Operation of the MFCs at Open-circuit Potential

The OCVs of the capacitive MFC (MFC_c) and the non-capacitive MFC (MFC_{nc}) as recorded with a data logger for 75 days and 7 hours are given in Fig. 3.
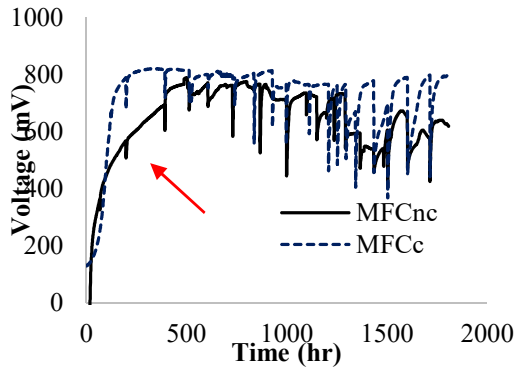
Fig. 3. Open-circuit potentials of capacitive and non-capacitive MFCs. The arrow indicates a typical point of polarisation and the first point of feeding

The initial starting voltages for the capacitive and non-capacitive MFCs were 128.5 ± 0.001 and -68 ± 0.023, respectively. The pattern of the graph mimics the growth curve typical of bacterial growth, but without the death phase. The absence of the death phase is apparently due to the occasional feeding of the MFCs with an additional substrate to keep the microbial activities in the stationary phase. The capacitive MFC (MFCc) reached a stationary phase after 269 hours, whereas it took slightly longer for the non-capacitive MFC (MFCnc), which reached stability only after 392 hours. The growth of OCVs from the lag phase to the stable phase is considered as microbial charging of the MFCs to full capacity. MFC_c and MFC_{nc} charged to OCVs of 789 mV and 567mV, respectively, after 197 hours before the first feeding, after which the OCVs increased to 818 ± 1.4 mV and 788 ± 8.5 mV for MFC_c and MFC_{nc}, respectively. The MFcs reached a fairly stable state around these OCVs, with the MFC_c showing better stability over an extended period of operation. Fig. 4. shows the behavior of the MFCs after Polarization.
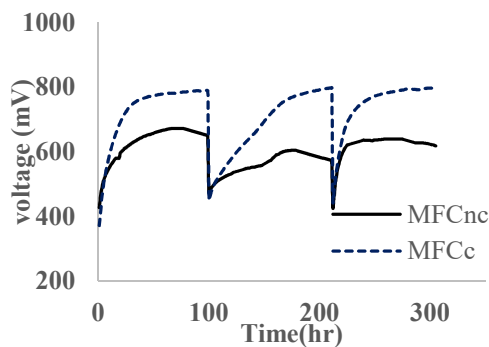

Fig. 4. Self-charging of MFCs after polarization

The last part of Fig. 3. is shown in Fig. 4. to demonstrate the self-charging of the MFCs to their steady-states after polarization. For both MFCs, the charging time was faster during the exponential phase, so the

polarization points are not obvious during this phase. The polarization points are evident from the stationary phase onward, showing that the time for the MFCs to self-charge increased as the MFCs operated around the stationary phase. MFC_c reached its steady open-circuit potential after each polarization in the stationary phase, in contrast to the MFC_{nc}, which exhibited irregular potential behavior. The difference in potential behaviors has been attributed to the storability of electrons produced by the microorganisms by the capacitive electrodes [19]

B. Electrochemical Performance of the Mfcs

1) Polarization analysis: To measure the performance of the MFCs, linear sweep voltammetry was performed at least every three days. Fig. 5. shows *typical* polarization and power curves of the two MFCs, while Fig. 6 shows the change in average maximum power during the first 63 days of operation.
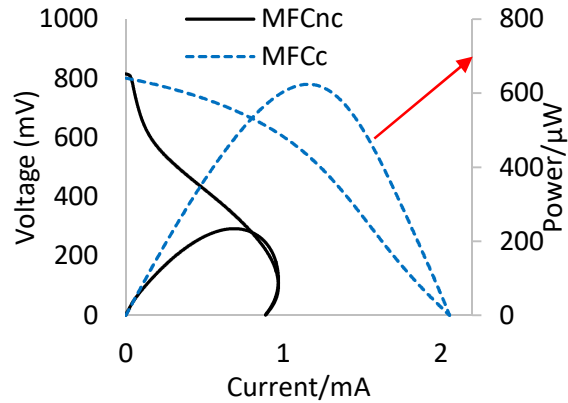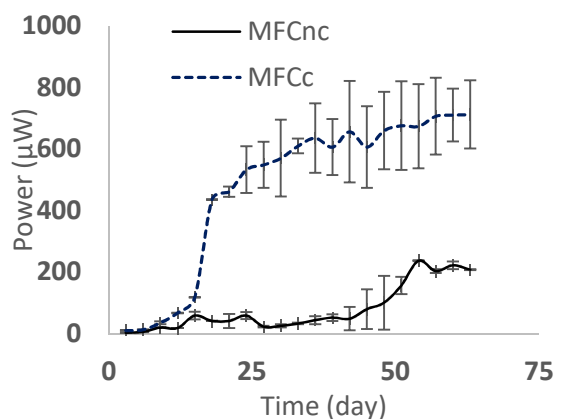

Fig. 5. Polarization and Power Curves of the MFCs

Fig. 6. Maximum Performance of the MFCs with time. Data points and error bars represent the mean $\pm$ standard deviation of the maximum power from the duplicate MFCs

The maximum power generated by MFC_c and MFC_{nc} respectively is 712.5 ± 110.8 µW and 236.5 ± 6.15 µW. As can be seen, the power of MFC_{nc} does not increase in the same proportion as the OCV. This is attributed

to a lack of charge storage capability of the MFCs. The overpotentials were higher than the cell voltage during polarization. For example, the best performance of one of the duplicates occurs at an OCV of 815mV, while the cell voltage and current at the point of maximum performance were 341 mV and 0.687 mA, respectively, resulting in a power of 234.3 uW. This means that 474mV accounted for the total overpotential (lost volt). When MFC_c reached a similar OCV of 813mV, the cell voltage at maximum power was 450mV at a current of 1.41mA, resulting in a power of 634.5 uW, which is about 3 times better performance. MFC_c had lower overpotentials and higher current, apparently due to the charge storage capability of the capacitive electrodes.

2) Impedance Spectroscopic analysis: To obtain more detailed information about the capacitance, ohmic, and charge transfer impedances of the MFCs, an EIS was performed on a whole-cell basis (two-electrode system). Fig. 7 and Fig. 8 show the Nyquist plot of MFC_c and MFC_{nc}, respectively.
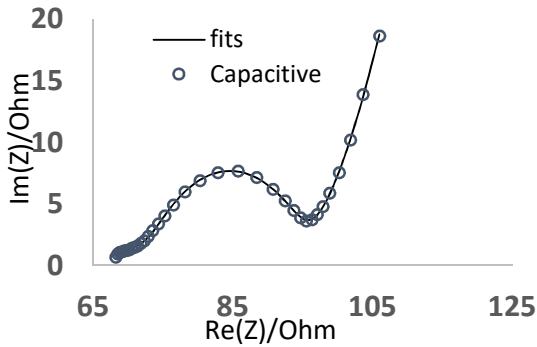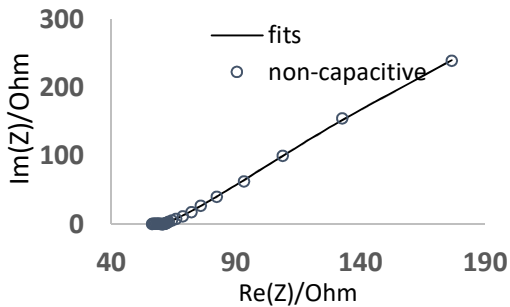

Fig. 7. Nyquist impedance plot of MFC_c

Fig. 8. Nyquist impedance plot of MFC_{nc}

Randle circuits were chosen for modeling the physical systems considering the kinetics of the Porous Electrodes in Presence of Redox Species. For Fig. 7., an equivalent electrical circuit R1+C2//R2+C3//R3+C4+W3 was chosen such that the double layer capacitances of anode and cathode C2 and

C3 were respectively, parallel to their corresponding resistances at the interface between the electrodes and the electrolyte. Besides, the diffuse layer capacitance at the coating/metal interface (C4) and the equivalent Wamburg impedance (W4) of the two electrodes were connected in series [40]. The absence of C4 in MFC_{nc} is obvious in Fig.8. Therefore, the same Randle circuit could not model the parameters for MFC_{nc}. The impedance parameters were modeled with C4 omitted. Table 1 shows the parameters modeled with the equivalent electrical circuits using EC-Lab V11.2

TABLE I.   IMPEDANCE AND CAPACITIVE PARAMETERS OF THE MFCs

Cells	R1 (Ω)	R+R3 (Ω)	C2//C3 (µf)	C4 (F)
MFCc	68.5	26.8	8.282	2.012
MFCnc	56.7	1791.5	5.034	

The parameters were obtained by simulating the electrochemical impedance spectroscopy to the equivalent circuits R1+C2//R2+C3//R3+C4+W3 and R1+C2//R2+C3//R3+W3, respectively. Where R1 is the total Ohmic resistance, R2 and R3 represent the charge transfer resistance of the anode and cathode respectively for each MFC. C2 and C3 respectively represent the double-layer capacitance of the anode and cathode. C4 is the equivalent capacitance of the coating/metal interface of the anode and cathode. C2 and C3 in the model were replaced with constant phase elements since the electrodes are not pure capacitors.

Since a two-electrode system was used, the equivalent double-layer capacitance of the anode and cathode and the equivalent capacitance of the coating/metal interface of the anode and cathode were represented by an equivalent capacitance of the series connection, as calculated from Equation 1

$$\frac{1}{c} = \frac{1}{c_a} + \frac{1}{c_c} \qquad (1)$$

Where C_a = anode capacitance, C_c = cathode capacitance. Also, the charge transfer resistance was considered as the sum of R2 and R3.

The ohmic resistance of MFC_c was slightly higher than that of MFC_{nc}, which is probably due to a difference in the conductivity of the bulk electrolyte at the measurement point. This is also an indication that the poor performance of MFC_{nc} was not due to the contact resistance between the electrodes and the current collectors, because the ohmic resistance is composed of the contact resistance, the resistance of the electrode material, and the resistance of the bulk electrolyte [41]. The large difference in charge transfer resistance explains the difference in electron transfer processes in the two MFCs. This implies that the application of the capacitive electrodes in the single chamber MFC significantly reduced the charge transfer resistance and thus improved the oxygen reduction reaction at the cathode. Therefore, the better performance of the MFC_c was attributed to the reduction of the charge transfer resistance and the pseudocapacitive properties of both

the anode and the cathode, which resulted in a higher specific energy of the MFC according to Equation 2 [26].

$$E_{max} = \frac{1}{2}\frac{(CV_{\max})^2}{m_{sc}} \qquad (2)$$

Where V_{max} is the maximum practical cell voltage, M_{sc} is the total electrode mass.

IV. CONCLUSION

The study compared the outputs of a capacitive and a non-capacitive MFC. The capacitive MFC generated a maximum power of 712.5 ± 110.8 µW, while the non-capacitive MFC generated 236.5 ± 6.15 µW during the study period. Impedance spectroscopy of the MFC showed that the capacitive properties of the electrodes resulted in better performance of the single-chamber MFC by reducing the charge transfer resistance and storing the charge generated by the electroactive bacteria. It was also found that the diffuse layer capacitance at the layer/metal interface of the electrodes contributed more to the capacitive properties of the MFC than the double-layer capacitance. Further investigation is needed to determine the specific contribution of each electrode to the total capacitance of the capacitive single-chamber MFC.

REFERENCES

[1] C. Santoro, X.A. Walter, F. Soavi, J. Greenman, I. Ieropoulos, Self-stratified and self-powered micro-supercapacitor integrated into a microbial fuel cell operating in human urine, Electrochimica acta 307 (2019) 241–252.

[2] T.H. Pham, P. Aelterman, W. Verstraete, Bioanode performance in bioelectrochemical systems: recent improvements and prospects, Trends in biotechnology (2009) 168–178.

[3] A.G. Capodaglio, D. Molognoni, E. Dallago, A. Liberale, R. Cella, P. Longoni et al., Microbial fuel cells for direct electrical energy recovery from urban wastewaters, TheScientificWorldJournal (2013) 634738

[4] J. You, J. Greenman, I. Ieropoulos, Novel Analytical Microbial Fuel Cell Design for Rapid in Situ Optimisation of Dilution Rate and Substrate Supply Rate, by Flow, Volume Control and Anode Placement, Energies 11 (2018) 2377.

[5] I. Simeon, O. A. R.aji, A. Gbabo, C. Okoro-Shekwaga, Performance of a Single Chamber Soil Microbial Fuel Cell at Varied External Resistances for Electric Power Generation, Journal of Renewable Energy and Environment 3 (2016).

[6] A.A. Yaqoob, M.N.M. Ibrahim, M. Rafatullah, Y.S. Chua, A. Ahmad, K. Umar, Recent Advances in Anodes for Microbial Fuel Cells: An Overview, Materials (Basel, Switzerland) (2020).

[7] B.E. Logan, B. Hamelers, R. Rozendal, U. Schröder, J. Keller, S. Freguia et al., Microbial fuel cells: methodology and technology, Environmental science & technology 40 (2006) 5181–5192.

[8] S. Bensaid, B. Ruggeri, G. Saracco, Development of a Photosynthetic Microbial Electrochemical Cell (PMEC) Reactor Coupled with Dark Fermentation of Organic Wastes: Medium Term Perspectives, Energies 8 (2015) 399–429.

[9] M. Di Lorenzo, K. Scott, T.P. Curtis, I.M. Head, Effect of increasing anode surface area on the performance of a single chamber microbial fuel cell, Chemical Engineering Journal 156 (2010) 40–48.

[10] S. Kalathil, S.A. Patil, D Pant. Microbial Fuel Cells: Electrode Materials. Encyclopedia of Interfacial Chemistry, Elsevier, 2018.

[11] M.H. Do, H.H. Ngo, W.S. Guo, Y. Liu, S.W. Chang, D.D. Nguyen, L.D. Nghiem, B.J. Ni, Challenges in the application of microbial fuel cells to wastewater treatment and energy production: A mini review, Science of The Total Environment 639 (2018) 910–920.

[12] J. R. Jambeck, Microbial Fuel Cells in Landfill Applications. Faculty of Engineering University of Georgia. EREF MFC Report 2-25-10.

[13] B.E. Logan, B. Hamelers, R. Rozendal, U. Schröder, J. Keller, S. Freguia et al., Microbial fuel cells: methodology and technology, Environmental science & technology 40 (2006) 5181–5192.

[14] D. Pocaznoi, A. Calmet, L. Etcheverry, B. Erable, A. Bergel, Stainless steel is a promising electrode material for anodes of microbial fuel cells, Energy Environ. Sci. 5 (2012) 9645.

[15] Y. Liang, H. Feng, D. Shen, N. Li, K. Guo, Y. Zhou et al., Enhancement of anodic biofilm formation and current output in microbial fuel cells by composite modification of stainless steel electrodes, Journal of Power Sources 342 (2017) 98–104.

[16] X.A. Walter, C. Santoro, J. Greenman, I. Ieropoulos, Self-stratifying microbial fuel cell: The importance of the cathode electrode immersion height, International journal of hydrogen energy 44 (2019) 4524–4532.

[17] M. Saadi, J. Pezard, N. Haddour, M. Erouel, T.M. Vogel, K. Khirouni, Stainless steel coated with carbon nanofiber/PDMS composite as anodes in microbial fuel cells, Mater. Res. Express (2020).

[18] M. Ghasemi, W.R.W. Daud, S.H.A. Hassan, S.-E. Oh, M. Ismail, M. Rahimnejad et al., Nano-structured carbon as electrode material in microbial fuel cells: A comprehensive review, Journal of Alloys and Compounds 580 (2013) 245–255.

[19] A. Deeke, T.H.J.A. Sleutels, H.V.M. Hamelers, C.J.N. Buisman, Capacitive bioanodes enable renewable energy storage in microbial fuel cells, Environmental science & technology (2012) 3554–3560.

[20] C. Donovan, A. Dewan, D. Heo, H. Beyenal, Batteryless, wireless sensor powered by a sediment microbial fuel cell, Environmental science & technology 42 (2008) 8591–8596.

[21] A. Dewan, C. Donovan, D. Heo, H. Beyenal, Evaluating the performance of microbial fuel cells powering electronic devices, Journal of Power Sources 195 (2010) 90–96.

[22] Y. Kim, M.C. Hatzell, A.J. Hutchinson, B.E. Logan, Capturing power at higher voltages from arrays of microbial fuel cells without voltage reversal, Energy Environ. Sci. 4 (2011) 4662.

[23] C. Santoro, M. Kodali, S. Kabir, F. Soavi, A. Serov, P. Atanassov, Three-dimensional graphene nanosheets as cathode catalysts in standard and supercapacitive microbial fuel cell, Journal of Power Sources 356 (2017) 371–380.

[24] J. Vidic, S. Stankic, F. Haque, D. Ciric, R. Le Goffic, A. Vidy et al., Selective antibacterial effects of mixed ZnMgO nanoparticles, Journal of nanoparticle research an interdisciplinary forum for nanoscale science and technology 15 (2013) 1595.

[25] K.R. Fradler, J.R. Kim, H.C. Boghani, R.M. Dinsdale, A.J. Guwy, G.C. Premier, The effect of internal capacitance on power quality and energy efficiency in a tubular microbial fuel cell, Process Biochemistry 49 (2014) 973–980.

[26] L. Caizán-Juanarena, C. Borsje, T. Sleutels, D. Yntema, C. Santoro, I. Ieropoulos et al., Combination of bioelectrochemical systems and electrochemical capacitors: Principles, analysis and opportunities, Biotechnology advances (2020) 107456.

[27] X. Chen, R. Paul, L. Dai, Carbon-based supercapacitors for efficient energy storage, National Science Review 4 (2017) 453–489.

[28] X. Wang, A. Hu, C. Meng, C. Wu, S. Yang, X. Hong, Recent Advance in Co3O4 and Co3O4-Containing Electrode Materials for High-Performance Supercapacitors, Molecules (Basel, Switzerland) 25 (2020).

[29] D. Zhao, K. Jiang, J. Li, X. Zhu, C. Ke, S. Han et al., Supercapacitors with alternating current line-filtering performance, BMC Mat 2 (2020).

[30] X. Peng, H. Yu, H. Yu, X. Wang, Lack of anodic capacitance causes power overshoot in microbial fuel cells, Bioresource technology (2013) 353–358.

[31] C. Borsje, D. Liu, T.H.J.A. Sleutels, C.J.N. Buisman, A. Ter Heijne, Performance of single carbon granules as perspective for larger scale capacitive bioanodes, Journal of Power Sources 325 (2016) 690–696.

[32] Z. Lv, D. Xie, F. Li, Y. Hu, C. Wei, C. Feng, Microbial fuel cell as a biocapacitor by using pseudo-capacitive anode materials, Journal of Power Sources 246 (2014) 642–649.

[33] C. Santoro, F. Soavi, A. Serov, C. Arbizzani, P. Atanassov, Self-powered supercapacitive microbial fuel cell: The ultimate way of boosting and harvesting power, Biosensors & bioelectronics (2016) 229–235.

[34] Y. Li, Y. Yan, H. Ming, J. Zheng, One-step synthesis Fe3N surface-modified Fe3O4 nanoparticles with excellent lithium storage ability, Applied Surface Science 305 (2014) 683–688.

[35] M.I. Simeon, F.U. Asoiro, M. Aliyu, O.A. Raji, R. Freitag, Polarization and power density trends of a soil - based microbial fuel cell treated with human urine, Int J Energy Res 44 (2020) 5968‑5976.

[36] M.I. Simeon, M.Y. Otache, T. A. Ewemoje., Application of urine as fuel in a soil-based membrane-less single chamber microbial fuel cell, CIGR Journal 21 (2019) 115–121.

[37] I.M. Simeon, A.L. Imoize and R. Freitag. Evaluation of the electrical performance of a soil-type microbial fuel cell treated with a substrate at different electrode spacings. In proceedings: International Conference on Energy, Environment and Storage of Energy, (ICEESEN 2020). 19th – 21th of November 2020 Kayseri, Turkey.

[38] Ran Mao, Chao Huang, Xu Zhao, Mei Ma, Jiuhui Qu., Dechlorination of triclosan by enhanced atomic hydrogen-mediated electrochemical reduction: Kinetics, mechanism, and toxicity assessment: Volume 241, February 2019, Pages 120-129, Applied Catalysis B: Environmental 241 (2019) 120–129.

[39] N.S. Ramaraja P Ramasamy, Electrochemical Impedance Spectroscopy for Microbial Fuel Cell Characterization, J Microbial Biochem Technol (2013).

[40] A. Lasia, Electrochemical Impedance Spectroscopy and its Applications, Springer New York, New York, NY, 2014.

[41] T. Nam, S. Son, E. Kim, H.V.H. Tran, B. Koo, H. Chai et al., Improved structures of stainless steel current collector increase power generation of microbial fuel cells by decreasing cathodic charge transfer impedance, Environmental Engineering Research 23 (2018) 383–389.